Equal Area Rule Methods for Ternary Systems†

Guor-Shiarn Shyu, Nishawn S. M. Hanif, Juan F. J. Alvarado, Kenneth R. Hall, and Philip T. Eubank*

Chemical Engineering Department, Texas A&M University, College Station, Texas 77843-3122

Eubank and Hall have recently shown the equal area rule (EAR) applies to the composition derivative of the Gibbs energy of a binary system at fixed pressure and temperature regardless of derivative continuity. A sufficient condition for equilibria, EAR is faster and simpler than either the familiar tangent-line method or the area method of Eubank et al. Here, we show that EAR can be extended to ternary systems exhibiting one, two, or three phases at equilibrium. A single directional vector is searched in composition space; at equilibrium, this vector is the familiar tie line. A sensitive criterion for equilibrium under EAR is equality of orthogonal derivatives such as $(\partial g/\partial x_1)_{x_2,P,T}$ at the end points (α and β), where $g \equiv (\Delta_m G/RT)$. Repeated use of the binary algorithm published in the first reference allows rapid, simple solution of ternary problems, even with hand-held calculators for cases where the background model is simple (e.g., activity coefficient models) and the derivative continuous.

Introduction

The phase equilibrium behavior of fluid mixtures is an important design consideration for both chemical processes and oil production. In chemical process design, for example, it is essential to know the thermodynamic properties, especially the number and composition of equilibrium phases for "staged" operations. For oil production proper modeling of reservoir processes requires the correct description of the number and composition of the different equilibrium phases present in the reservoir.

The *K*-value method and Gibbs energy minimization (GEM) methods are techniques generally used for phase equilibrium calculations (Ammar and Renon, 1987). The first procedure solves simultaneously a set of material balances and thermodynamic equations. The second procedure minimizes the Gibbs energy with respect to the composition of the different components in the mixture. Both procedures can employ a variety of background models. These include (1) an equation of state/mixture combining rule (EOS/MCR) model, (2) the gamma/phi method with different models and MCR for the gas and liquid, and (3) molecular-based models.

The usual engineering approach for solving phase equilibrium problems is to use the *K*-value procedure. However, this procedure may fail to predict the correct number of phases or it may provide trivial solutions (all phases present having identical properties). It is important to understand that this is a fault of the *procedure* and not of the underlying *model*. Both the procedure and the model can provide significant deviations from experiment. While it may be difficult to improve a G^E model or an EOS/MCR model, we can fix the procedure problem by using *Gibbs energy minimization techniques*. When a computer graphs the three-dimensional Gibbs surface, $G(P,T,z)$ for binary systems, it becomes apparent where and why *K*-value procedures fail. The failure occurs because the initial guess in the iterative procedure causes the simulator to converge at a local Gibbs energy minimum, not a global minimum. Given the number of minima appearing on the Gibbs surface, *K*-value procedures can converge to solutions which yield an incorrect number of phases and even the wrong phase identification. The problem is that more than one solution exists, each satisfying equality of fugacities. However, only one exists that minimizes the total Gibbs energy (the global minimum) and thus satisfying the second law of thermodynamics and nature.

K-value procedures usually succeed, even with poor initial guesses, for binary systems that exhibit only vapor–liquid equilibria. However, false equilibria usually result near the three-phase pressure line for vapor–liquid–liquid binaries as first demonstrated by Baker et al. (1982) for CO_2/*n*-decane near 248 K. As the number of components increase, the possibility of additional fluid phases also increases as does the likelihood of obtaining false equilibria from the *K*-value method, necessitating increased use of a Gibbs minimization technique.

Techniques using Gibbs energy minimization (GEM) for solving phase equilibrium problems from basic thermodynamic formula are common (Heidemann, 1974; Gautam; Seider, 1979; Trangenstein, 1985; Cairns and Furzer, 1990). Two principal algorithms are used in this method: the tangent-line procedure (Michelsen, 1982a,b) which minimizes the vertical distance from the tangent line to the Gibbs energy surface, and the area method (Eubank et al., 1992) which searches for the equilibrium points by integrating the Gibbs energy curve. Alvarado (1993) has simplified the procedure for the area method and has reduced its required computer time.

Eubank and Hall (1995) have shown recently that the tangent-line criterion reduces to an equal area construction for the derivative of the total Gibbs energy plotted against composition. A new algorithm was tested on some binary systems and has the advantages of easy implementation and fast convergence. In this paper, we generate a more general procedure and apply this method to ternary systems, including two- and three-phase systems. To maintain rigor, the entire composition space must be checked for any Gibbs minimization procedure. Here we thus calculate the entire diagram as a matter of course. EAR holds a decided advantage over the tangent-lines method for calculations near critical points, at critical end points, and in the retrograde region due to its added sensitivity. Indeed, EAR was first used by Hicks and Young (1977) to determine binary vapor–liquid critical loci.

† Presented at the Spring Meeting of the AIChE, Houston, TX, March 20, 1995.

* Author to whom correspondence should be addressed.

0888-5885/95/2634-4562$09.00/0

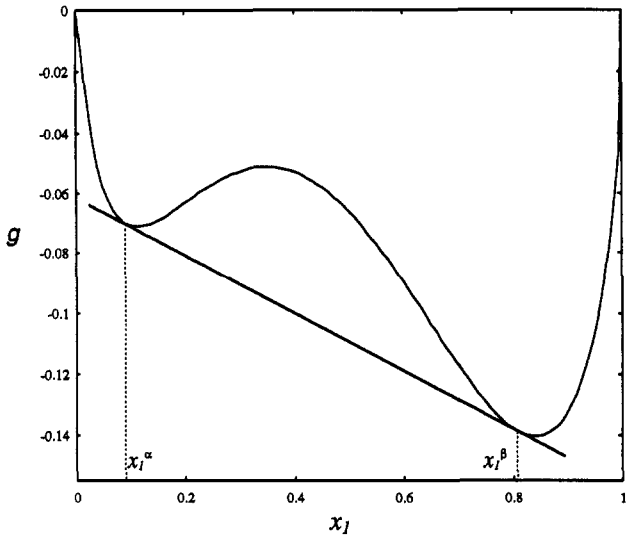

Figure 1. Typical plot of g versus x_1. Here $g \equiv (\Delta_m G/RT)$.

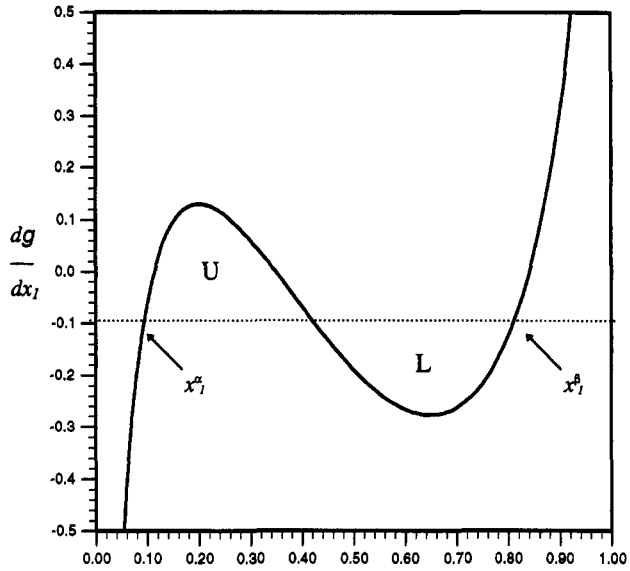

Figure 2. Typical plot of (dg/dx_1) versus x_1. Here $g \equiv (\Delta_m G/RT)$.

Equal Area Rule

For a pure component, the Maxwell equal area rule (MEAR) is a basic construct for determining saturated phase volumes from equations of state. The fundamental principle is that when a horizontal line drawn through the trace of a subcritical isotherm on a pressure/volume diagram equalizes the areas of the *van der Waals loop,* above and below the line, it intersects the isotherm at the saturated volumes. The lowest volume root is the saturated liquid, the highest root is the vapor, and the middle root is mechanically unstable and thus discarded. For a binary mixture, another basic construct exists which determines the phase compositions by establishing the tangent line to the total Gibbs energy curve plotted against composition. Eubank and Hall (1994) demonstrated that finding the tangent line also reduces to an equal area construction for the derivative of the total Gibbs energy plotted against composition.

To illustrate the binary solution problem, Figure 1 provides a plot of the dimensionless Gibbs energy of mixing, $g \equiv (\Delta_m G/RT)$ against x_1 whereas Figure 2 presents a typical plot of $(\partial g/\partial x_1)_{T,P}$ against x_1. In both diagrams, x_1^α and x_1^β are the corresponding equilibrium

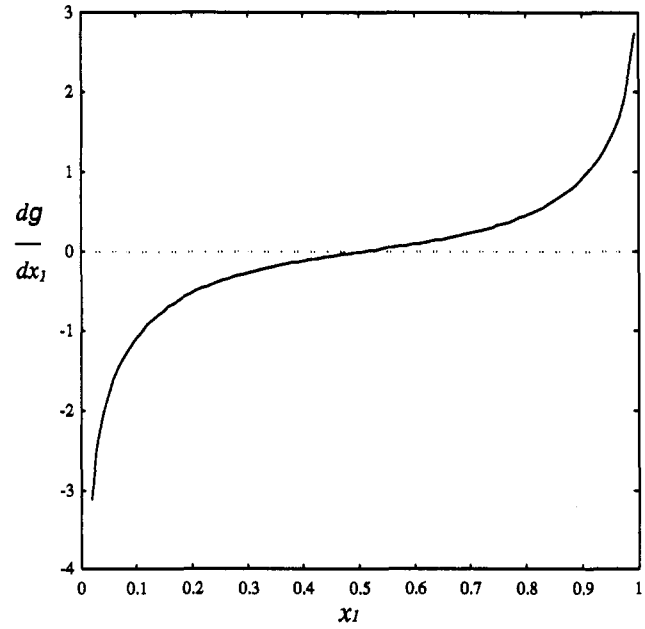

Figure 3. Typical plot of (dg/dx_1) versus x_1 with no phase splitting. Here $g \equiv (\Delta_m G/RT)$.

compositions. If no van der Waals loops appear, the system is stable with one phase. Figure 3 shows such an example.

In Figure 1, the equilibrium compositions result from satisfying the tangent-line criterion:

$$\left(\frac{\partial g}{x_1}\right)_{T,P}^{\alpha} = \left(\frac{\partial g}{\partial x_1}\right)_{T,P}^{\beta} = \frac{g^\beta - g^\alpha}{x_1^\beta - x_1^\alpha} \equiv g_1' \qquad (1)$$

Eubank and Hall (1995) derive the equation behind the equal area rule described by eq 1:

$$\int_{x_1^\alpha}^{x_1^\beta}\left(\frac{\partial g}{\partial x_1}\right)_{T,P} dx_1 = g^\beta - g^\alpha = g_1'(x_1^\beta - x_1^\alpha) \qquad (2)$$

where x_1^α and x_1^β are the equilibrium compositions and g_1' is the value of $(\partial g/\partial x_1)_{T,P}$ at the equilibrium condition. In Figure 2, equilibrium occurs at the value of g_1' which equalizes the upper area U and the lower area L.

Eubank and Hall (1995) developed an algorithm, which normally converges in one to three iterations, for equal area problems assuming a reasonable, if not accurate, initial guess. The procedure is to guess an initial g_1' and then to calculate the phase compositions and to adjust g_1' using

$$(g_1')_{k+1} = \frac{\left[\int_{x_1^\alpha}^{x_1^\beta}\left(\frac{\partial g}{\partial x_1}\right)_{T,P} dx\right]_k}{[x_1^\beta - x_1^\alpha]_k} \qquad (3)$$

The procedure described above is summarized as follows:

1. Check for the existence of van der Waals loops by determining cusp or inflection points along the Gibbs energy path. If no cusp or less than two inflection points exist, the system exhibits no phase splitting; if a cusp or inflections exist proceed to steps 2–5.

2. Choose an initial value of $(g_1')_0$ by calculating the average value of the two extremes in Figure 2.

Table 1. Equal Area Rule Applied to a Binary System with $G^E/RT = x_1x_2(2.5x_2 + 1.3x_1)^a$

iteration step k	$(g_1')_k$	$(x_1^\alpha)_k$	$(x_1^\beta)_k$	$\lvert(g_1')_k - (g_1')_{k+1}\rvert$
0	−0.261 16	0.151 6	0.576 50	3.846×10^{-3}
1	−0.265 01	0.149 1	0.571 90	9.319×10^{-6}
2	−0.265 01	0.149 08	0.571 88	6.204×10^{-11}

[a] The initial value of g_1' is calculated by the average of two extremes, −0.219 42 and −0.302 88.

3. Find the corresponding compositions $(x_1^\alpha)_k$ and $(x_1^\beta)_k$ at $(g'_1)_k$ where "k" denotes the iteration number.
4. Calculate $(g'_1)_{k+1}$ using eq 3.
5. Check convergence by comparing the difference between $(g'_1)_k$ and $(g'_1)_{k+1}$. If the difference is less than an acceptable tolerance (such as 1×10^{-8}), then the corresponding compositions are the equilibrium compositions. Otherwise, use the new $(g'_1)_{k+1}$ and return to step 2 and repeat until convergence.

Table 1 contains an example which calculates the Gibbs energy of mixing using the Margules equation:

$$\frac{G^E}{x_1x_2RT} = Ax_2 + Bx_1 \tag{4}$$

and provides the Gibbs energy of mixing as

$$g \equiv \frac{\Delta_m G}{RT} = x_1x_2(Ax_2 + Bx_1) + x_1 \ln x_1 + x_2 \ln x_2 \tag{5}$$

Only three iterations are needed to achieve convergence, as can be seen in Table 1.

Extension to Ternary Systems

Applying the equal area rule to ternary systems requires one additional consideration, following the tie-line vector procedure of Eubank et al. (1992). This procedure was later used by Kao (1992, 1995), who termed it the "separation vector formulation". At constant temperature and pressure, the restriction on mole fraction ($\sum x_i = 1$) implies that the Gibbs energy of mixing depends upon only two variables, the mole fractions x_1 and x_2 :

$$g = g(x_1,x_2) \tag{6}$$

Figure 4 illustrates that the compositions of the two phases at equilibrium are connected by a straight line which passes through the overall composition of the mixture (z_1, z_2) and satisfies the material balances as in a standard flash calculation. At equilibrium, the relative change between two components at the overall composition (z_1, z_2) along a tie line is a constant. Let us define the relative change function (D_{ij}) for components (i, j) at an overall composition (z_i, z_j) along a tie line as

$$D_{ij} \equiv \frac{dx_j}{dx_i} = \frac{x_j - z_j}{x_i - z_i} \quad (i \neq j) \tag{7}$$

For binary systems, $D_{12} = -1$, whereas for general multicomponent systems,

$$\sum_{\substack{j=1 \\ j\neq i}}^{c} D_{ij} = -1 \tag{8}$$

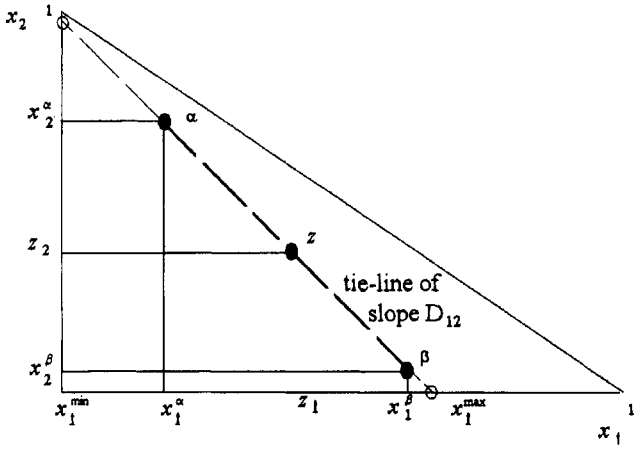

Figure 4. Triangular phase diagram for a ternary system. The equilibrium composition is obtained by searching for the equilibrium D_{12}. At a certain D_{12}, x_1 is bounded by two limits x_1^{max} and x_1^{min}.

In ternary systems, D_{ij} is the slope of a tie line. If D_{ij} and the overall compositions, [z_i], are available *a priori*, x_2 and x_3 can be replaced by x_1 as

$$x_2 = D_{12}(x_1 - z_1) + z_2 \tag{9}$$

$$x_3 = D_{13}(x_1 - z_1) + z_3 \tag{10}$$

where

$$D_{12} + D_{13} = -1 \tag{11}$$

Substituting eqs 8, 9, and 11 into eq 6, the Gibbs energy for a ternary system becomes

$$g = g(x_1,D_{12}) \tag{12}$$

Because the tie-line slope D_{12} is one of the unknowns for which we would like to solve, how do we find the equilibrium D_{12}? To determine the equilibrium $D_{12} \equiv D_{12}^e$ using EAR, we note that $g(x_1,x_2)$ so that

$$dg = g'_1(dx_1) + g'_2(dx_2) \tag{13}$$

where $g'_1 \equiv (\partial g/\partial x_1)_{x_2}$ and $g'_2 \equiv (\partial g/\partial x_2)_{x_1}$. Further,

$$(dg/dx_1) = g'_1 + g'_2D_{12}; \quad (dg/dx_2) = g'_1/D_{12} + g'_2 \tag{14}$$

We start the numerical search for D_{12}^e by choosing an initial value of D_{12} (e.g., $D_{12} = -1$). The model provides an equation for (dg/dx_1) as a function of x_1, D_{12} and (z_1, z_2). The variable x_1 along an assumed tie line is bounded by two limits depending on the slope D_{12} and the overall composition (z_1, z_2). One should calculate these two limits (x_{1min}, x_{1max}), which do not depend upon the model of Gibbs energy, by checking the condition ($0 < x_1, x_2, x_3 < 1$) being satisfied before calculating the Gibbs energy along the assumed tie line. In Figure 4, the open circles represent these two limits at this certain slope and the equilibrium points are searched inside this domain. When the third component disappears, the system becomes a binary system and the slope is −1. We can thus treat the binary system as a special case of this method.

Any assumed tie-line slope D_{12} near D_{12}^e when substituted into eq 14 causes the van der Waals loop to appear. However, if the assumed tie line is far from the equilibrium condition, no loops appear. Figure 5

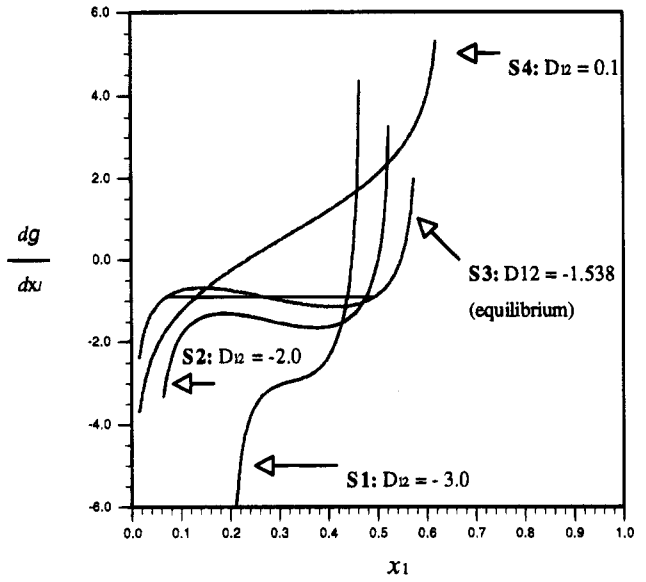

Figure 5. Representation of the relations between the van der Waals loop and D_{12}. Here $g \equiv (\Delta_m G/RT)$. If an assumed D_{12} is too large or too small, then no loop will occur, like curves S1 and S4. This diagram was prepared using a LLE model, $G^E/RT = 3.2x_1x_2 + 1.5x_1x_3$, and the input overall composition of $z_1 = 0.35$ and $z_2 = 0.35$.

shows typical loops appearing using different assumed slopes D_{12}. S1 and S4 are the lines from D_{12} far from D_{12}^e: one (S1) is calculated by a too-large D_{12} and the other one (S4) is calculated by a too-small D_{12}. No equal area loops occur in these two cases. However, S2 is from a value of D_{12} which is closer to the equilibrium condition. The equal area loop then appears. Finally the curve S3 is the converged, equilibrium value of D_{12}. It is thus obvious from an interactive computer graphic when the vicinity of D_{12}^e is approached. Simply put, the search for D_{12}^e has two stages: (1) a coarse-grid search for the van der Waals loop region and (2) a fine-grid search for D_{12}^e within this region. It is not necessary to use an interactive computer graphic to perform the course-grid search with EAR; one only needs to find loops (Figure 5) with a maximum and a minimum, a van der Waals loop. These extrema can be found numerically without graphics.

The fine-grid search for D_{12}^e is conducted with the convergence criteria that

$$(dg/dx_1)^\alpha = (dg/dx_1)^\beta \qquad (15)$$

is a necessary condition for equilibrium condition for equilibrium along the D_{12} pathway. However, this condition is not sufficient. Sufficiency is obtained by checking equality of the orthogonal derivatives

$$(g_1')^\alpha = (g_1')^\beta \quad \text{and} \quad (g_2')^\alpha = (g_2')^\beta \qquad (16)$$

and further checking to ensure that the D_{12} tie line is not cutting through the $g(x_1,x_2)$ surface at some other x_1 outside (x_1^α, x_1^β). The latter check is automatic when using EAR with a computer graphic that will display x_1 from $x_{1\min}$ to $x_{1\max}$. Our EAR procedure then provides a sufficient condition for correct final phase equilibria. Numerical experience shows that eq 16 is much more sensitive than eq 15. Satisfaction of both equalities of eq 16 provides eq 15, of course, through eq 14.

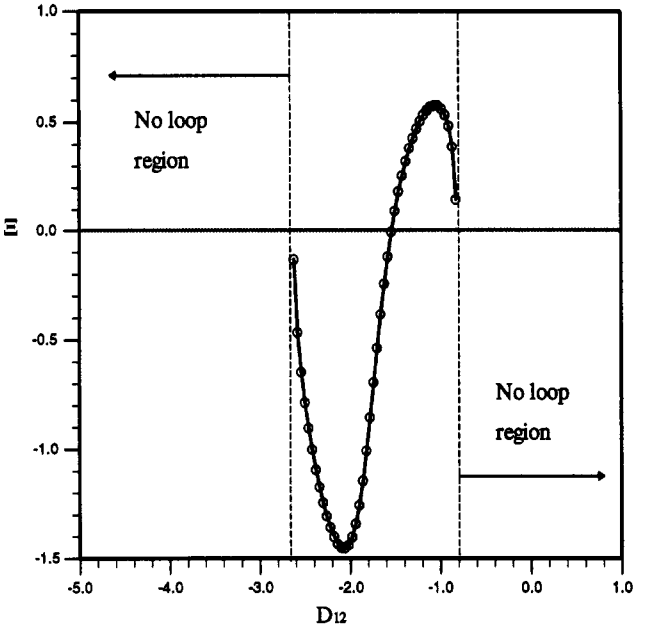

Figure 6. Plot showing the distribution of Ξ versus D_{12} in two-phase region. If an assumed D_{12} is too large or too small, then no loop will occur. The equilibrium D_{12}^e is obtained when Ξ approaches zero. In this case D_{12}^e is −1.538. This diagram was prepared using a LLE model, $G^E/RT = 3.2x_1x_2 + 1.5x_1x_3$, and the input overall composition of $z_1 = 0.35$ and $z_2 = 0.35$.

Table 2. Calculation Example for Ternary System by Using the Excess Energy Model: $G^E = 2.5x_1x_2 + 1.8x_1x_3 + 1.9x_2x_3$[a]

iteration step j	D_{12}	Ξ function	$(x_1^\alpha)_j$	$(x_1^\beta)_j$
1	−1.000 00	6.970×10^{-2}	0.250 71	0.599 30
2	−1.028 15	5.696×10^{-5}	0.243 77	0.589 41
3	−1.028 17	5.953×10^{-9}	0.243 778	0.589 40

[a] The overall compositions is located at ($z_1 = 0.425$, $z_2 = 0.425$).

A different function is now defined for numerical convergence under eq 16):

$$\Xi = \sum_{i=1}^{2} \left[\left(\frac{\partial g}{\partial x_i} \right)_{x_j}^{\alpha} - \left(\frac{\partial g}{\partial x_i} \right)_{x_j}^{\beta} \right] \quad (j \neq i; j \neq 3) \qquad (17)$$

Here, we seek the equilibrium compositions by searching the tie-line slope D_{12} to make Ξ less than a tolerance value (here 1×10^{-7}). Since Ξ depends only upon the slope D_{12} in a ternary system, it is very easy to find using any root searching procedure (e.g,, Newton−Raphson or the bisection method). Figure 6 shows the Ξ function calculated by a Margules-type model for the excess Gibbs energy versus the assumed slope D_{12}. In this case, the equilibrium D_{12} is −1.583.

An example for a ternary system calculated by the Margules-type excess energy model at an overall composition of ($z_1 = 0.425$, $z_2 = 0.425$) is given in Table 2.

To summarize the above procedure, we call the D_{12} searching procedure the external procedure whereas the equal area rule for searching g_1' is termed the internal procedure. The overall procedure is outlined as follows for a flash calculation with known overall composition (z_1, z_2):

1. Assume D_{12}.
2. Calculate the limits ($x_{1\min}$, $x_{1\max}$), as before for this certain D_{12}.

3. Transform x_2, x_3 to a function of x_1 and D_{12}.
4. Do the equal area rule procedure (internal procedure) inside the domain (x_{1min}, x_{1max}). If the equal area loop exists, then check the Ξ function. If no equal area rule loop exists for any D_{12}, then this system is considered as stable and only one phase exists.
5. If the Ξ function is less than the presumed tolerance value, then an equilibrium condition is achieved. Otherwise adjust D_{12} and repeat steps 2–5 until convergence.
6. Calculate x_2 and x_3 by the converged D_{12} and x_1. These compositions are thus equilibrium compositions.

Phase Composition Locus Calculations in Ternary Systems

As shown in the above section, the slope D_{12} is the key to solving for ternary system compositions. The initial value of D_{12} affects the convergence speed of this method. Fortunately, D_{12} can be reasonably estimated by extrapolating from the binary D_{12} of -1 when this binary exhibits phase splitting. In the phase composition locus calculation for ternary systems, we start the calculation from the binary boundary and then increase the composition of the third component from the dilute region to the more concentrated region. In this fashion we start from the sides of the composition triangle (see Figure 7) and work toward the interior.

When a new overall composition is set for calculating the equilibrium composition, the new initial D_{12} is extrapolated from the previous two converged D_{12}^e for the previous two overall compositions. The linear extrapolating equation used in this work is simply

$$(D_{12})_n = (D_{12})_{n-1} + [(D_{12})_{n-1} - (D_{12})_{n-2}] \quad (18)$$

where n is the number of separate flash calculations.

We calculate the new overall composition based upon the previously calculated midpoint, an average of equilibrium compositions, using

$$z_1 = (x_1)_{mid} + \Delta z_1 \quad (19)$$

$$z_2 = (x_2)_{mid} - \Delta z_1/D_{12}^e \quad (20)$$

$$z_3 = 1 - z_1 - z_2 \quad (21)$$

Figure 7 shows that eqs 19–21 produce a path line of overall compositions corresponding to the rectilinear line (Rowlinson and Swinton, 1982). When the line is straight all the way to the liquid–liquid critical point (plait point), the law of rectilinear diameters is obeyed. Otherwise, this numerical procedure produces a series of jointed straight lines each of a slope of $-(1/D_{12}^e)$, where D_{12}^e is from the previously equilibrium determination under EAR. That is, each new straight-line segment is drawn out of the midpoint of the previous equilibrium tie line with a slope normal to it. The increment Δz_1 is arbitrary and may be replaced by

$$\Delta z_2 = -(\Delta z_1/D_{12}^e) \quad (22)$$

when D_{12}^e is small causing Δz_1 to be insensitive compared to Δz_2. This procedure ensures calculation of the locus by using overall compositions inside the phase-splitting region.

Four types of ternary equilibria were studied. Figure 8 shows the general diagrams for those four types. In

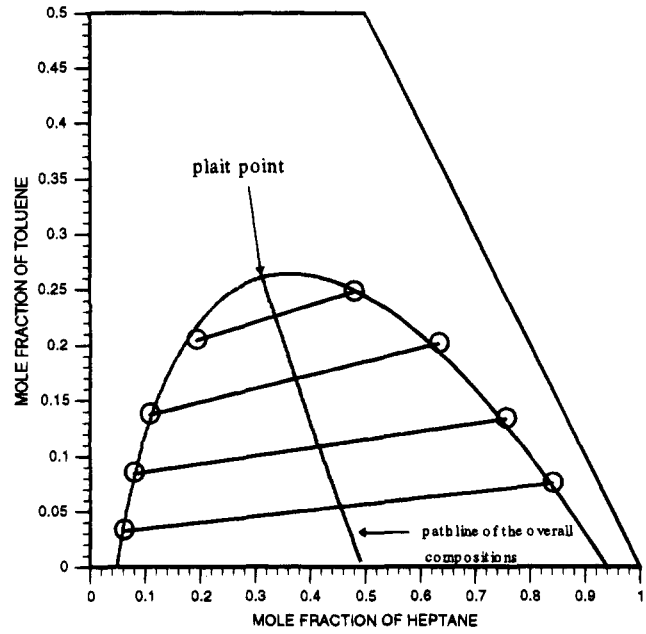

Figure 7. Phase diagram for heptane (1)/toluene (2)/aniline (3) at T = 20 °C. The path line of overall compositions is shown as the line inside the two-phase region. Circles are from the experimental data of Durandet and Gladel (1954), which is reported in Sørensen and Arlt (1977).

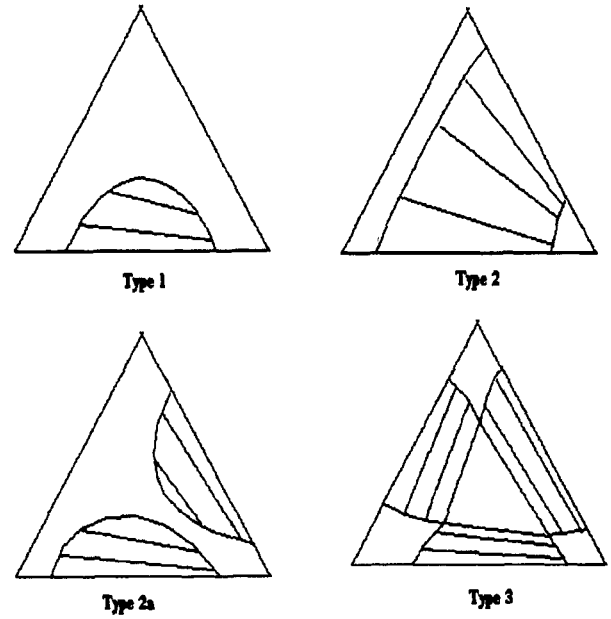

Figure 8. Types of ternary systems used in this article.

type 1, there is only one two-phase region and it has a single binary system boundary. In types 2 and 2a, there are two binary systems exhibiting phase splitting. For type 2 there is a single two-phase region for the ternary system whereas for type 2a there are two distinct two-phase regions. In types 3 and 3a, all three binary pairs exhibit phase splitting. In type 3, there exists one three-phase region whereas in type 3a (unshown), like type 2a, the two-phase regions are bounded by a continuous single-phase region. Other general types of ternary diagrams exist (Walas, 1985) but are not so common.

The above procedure is a general approach for calculating the phase locus from only one binary system boundary. Types 2, 2a, 3, and 3a can be calculated by using, repeatedly, the above procedure. In order to know how many phase-splitting regions are in the entire system, we check the three binary system boundaries

Table 3. Types and Parameters in Ternary Systems with Margules Models

Figure	type	a_{12}	a_{13}	a_{23}
12	2a	2.3	2.4	1.8
13	3	2.8	3.4	2.5
14	3	3.6	2.4	2.3

Table 4. Types and Parameters in Ternary Systems with NRTL Models[a]

i	j	α_{ij}	τ_{ij}	τ_{ji}
		Type 1; Heptane (1)/Toluene (2)/Aniline (3) at T = 20 °C[b]		
1	2	0.2	−0.311 24	−1.054 1
1	3	0.2	1.786 97	2.107 59
2	3	0.2	−0.213 18	0.054 19
		Type 2; Hexane (1)/Methylcyclopentane (2)/Aniline (3) at T = 34.5 °C[c]		
1	2	0.2	−0.550 10	0.394 24
1	3	0.2	1.787 03	1.440 14
2	3	0.2	1.515 85	0.906 51

[a] Parameters in both systems are recalculated from DECHEMA Data Series, Vol. V, Part 2. [b] Experimental data are from Durandet and Gladel (1954) in Sørensen and Arlt (1977). [c] Experimental data are from Darwent and Winkler (1943) in Sørensen and Arlt (1977).

first. If phase splitting occurs on a binary system boundary, we consider that one phase-splitting region can be calculated by starting from that binary system boundary. Once the number of phase-splitting boundaries is determined, the above procedure can be used repeatedly from each boundary. If there are more than two binary phase-splitting boundaries, three-phase phenomena should be considered. When the three binary pairs are completely miscible, but a two-phase island exists in the interior of the ternary triangle, our procedure must be modified to sweep the interior starting from selected ternary overall composition points.

Three-phase behavior exists when the two-phase loci from different starting points (different binary system boundaries) intersect each other. The three-phase composition is then obtained by finding the composition of the intersections. The reason why these intersections correspond to three-phase compositions is that all of these three points have the same gradient, which satisfies the tangent-plane criteria.

Results and Discussion

Tables 3 and 4 show the cases studied in this work. Two types of excess Gibbs models are used in this work. One is a simple symmetric form for the binary pair:

$$(G^E/RT) = a_{12}x_1x_2 + a_{13}x_1x_3 + a_{23}x_2x_3 \qquad (23)$$

where a_{12}, a_{13}, and a_{23} indicate the strength of the unlike pair repulsion. The other is the NRTL model (Renon and Prausnitz, 1965):

$$(G^E/RT) = \sum_i x_i \frac{\sum_j x_j\tau_{ji}h_{ji}}{\sum_k x_k h_{ki}} \qquad (24)$$

with

$$h_{ij} = \exp(-\alpha_{ij}\tau_{ij}); \quad (\alpha_{ij} = \alpha_{ji}) \qquad (25)$$

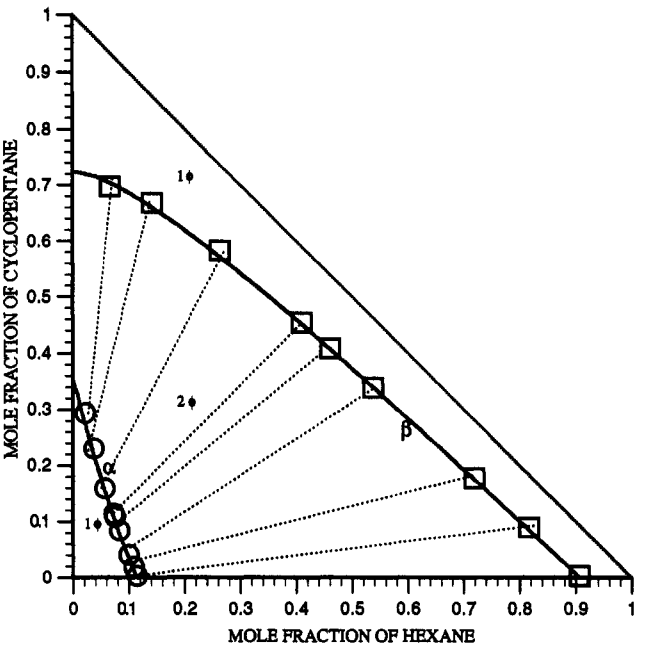

Figure 9. Phase diagram for hexane (1)/cyclopentane (2)/aniline (3) system at 34.5 °C. Solid lines are from data calculated by this work whereas circles and rectangles are from the experimental data of Darwent and Winkler (1943), which is reported in Sørensen and Arlt (1977). The α and β represent the index for each phase.

Table 3 shows the parameters used with eq 23 whereas Table 4 shows the parameters used with the NRTL model.

Figure 7 shows results for the heptane/toluene/aniline system (type 1) at 20 °C from the NRTL model. Parameters and experimental data are cited from the DECHEMA Chemical Data Series (Sørensen and Arlt, 1977). The line inside the two-phase region is the locus line of the overall compositions used for the calculations; it is calculated from eqs 19−22. The results in Figure 7 approach the plait point in a correct manner.

Figure 9 shows results for the hexane/cyclopentane/aniline system (type 2) at 34.5 °C. Phase-splitting behavior occurs at two binary system boundaries, cyclopentane/aniline and hexane/aniline. The starting point of the overall composition from each of the above boundaries predicts the same locus. Figure 10 shows the distribution ratio for cyclopentane, $N_2 \equiv (x_2^\beta/x_2^\alpha)$, in the two phases, which confirms that the slopes of tie lines from the cited model and this method are consistent with experimental data. Figure 11 shows results for a type 2a case using eq 23 as the model. Two different starting points predict the existence of phase-splitting behavior for the two separate regions.

Figures 12 and 13 show three-phase behavior in systems at constant temperature and pressure. Both diagrams are calculated using eq 23 as the model. As shown by Figures 12 and 13, starting the calculation from the three binary boundaries will cause the loci to intersect each other. Before the lines intersect each other, there is two-phase behavior inside the phase-splitting region and one-phase behavior outside the phase-splitting region. When the locus lines cross each other, the predicted lines become metastable lines instead of stable equilibrium lines. To confirm that this method was correctly predicting the three-phase compositions, conventional flash calculations were used for comparison. The circles in Figures 12 and 13 were calculated by solving simultaneously the equations for activity equality and restrictions of mole fractions ($\sum x_i$

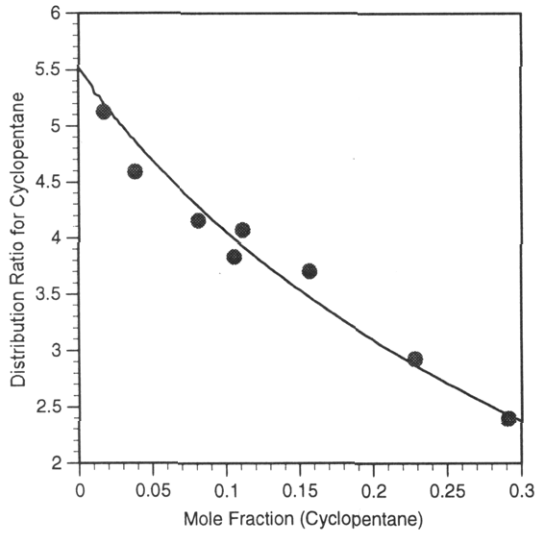

Figure 10. Distribution ratio, $N_2 \equiv (x_2^\beta/x_2^\alpha)$, for cyclopentane (2) at hexane (1)/cyclopentane (2)/aniline (3) at 34.5 °C. Circles are from the experimental data of Darwent and Winkler (1943), which is reported in Sørensen and Arlt (1977).

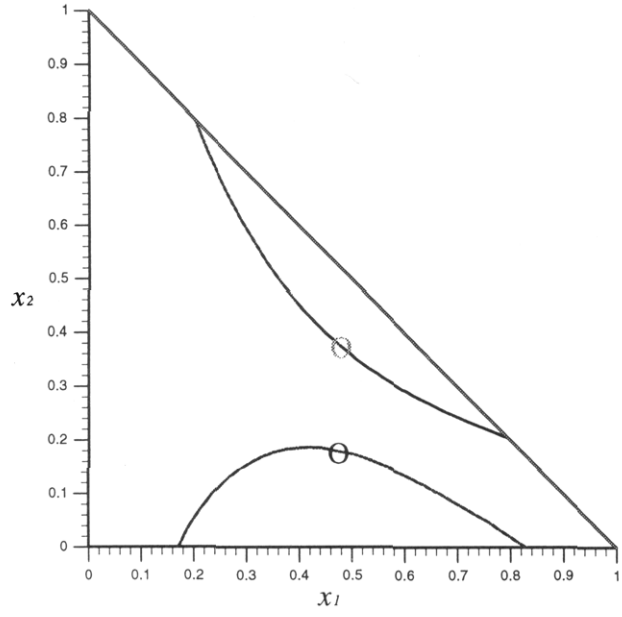

Figure 11. Diagram of a type 2a case. This diagram is calculated using a Margules-type model, eq 20, with $(G^E/RT) = 2.3x_1x_2 + 2.4x_1x_3 + 1.8x_2x_3$. The two circles represent the plait points.

$= 1$, $i = 1-3$). Consistency between the three-phase points obtained by the present method (EAR) and the circles was excellent. Heidemann (1983) noted that, when the same thermodynamic model is used to described different phases, it is possible that compositional computations by conventional methods may fail—they converge to the so-called "trivial solution" (the same composition value are obtained in different phases). The success of the calculation by conventional methods, however, depends upon the initial guess. When one does the calculation by conventional flash techniques for LLLE in Figures 12 and 13, the domain of convergence for the trivial solution is large, and thus it is easy to obtain the "trivial solution". Figures 12 and 13 show the advantage of EAR for obtaining three-phase composition safely and easily. Another important advantage of the present method with EAR is that we reduce the degrees of freedom of the search variables. Here, we only search for one D_{12} and then use EAR to find the corresponding compositions. While the D_{12} procedure works especially well with EAR, it was originally devised for use with the area method (Eubank et al., 1992), and we find that it improves the convergence speed of our tangent-line programs, as it eliminates the need to search for the tangent plane (ternary) or hyperplane ($C \geq 4$).

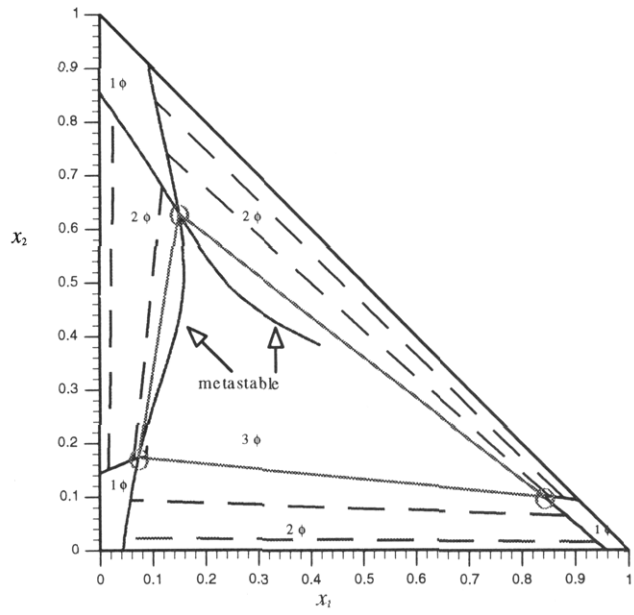

Figure 12. Results for a three-phase case. Equation 23 was used as the model with $a_{12} = 2.8$, $a_{13} = 3.4$, and $a_{23} = 2.5$. Three-phase compositions for (x_1, x_2) are obtained at (0.07387, 0.17307), (0.84168, 0.1002), (0.1491, 0.629).

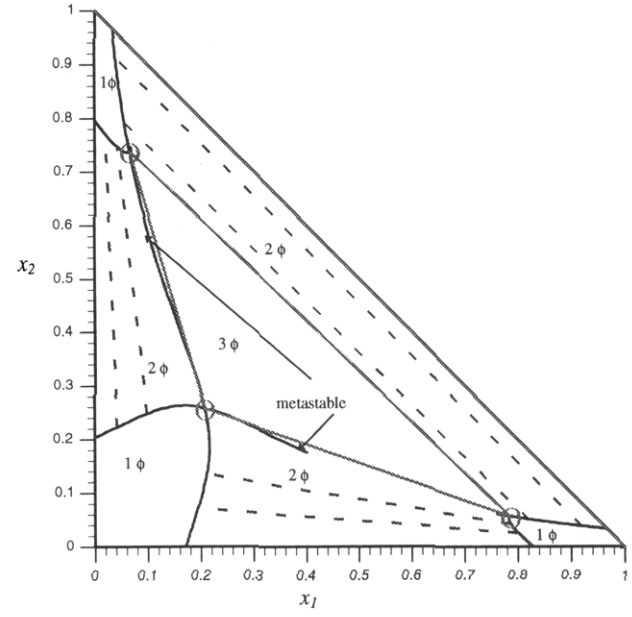

Figure 13. Results for a second three-phase case. Equation 23 was again used as the model but with $a_{12} = 3.6$, $a_{13} = 2.4$, and $a_{23} = 2.3$. The three-phase compositions for (x_1, x_2) are obtained at (0.7861, 0.05682), (0.0652, 0.7389), (0.2077, 0.2582).

Figure 14 shows the path lines of D_{12} with x_1 during the calculation procedure; the three lines result from starting at a different binary-pair boundary. All three lines start from $D_{ij} = -1$. In this work, we find that when D_{12} is larger than -0.1 (and less than 0) or D_{12} is less than -10, the convergence speed will become slow. However, when D_{12} is located inside those regions, the calculated line is already inside a metastable region. Thus, when D_{12} become larger than -0.1 or D_{12} becomes less than -10, we stop the calculation.

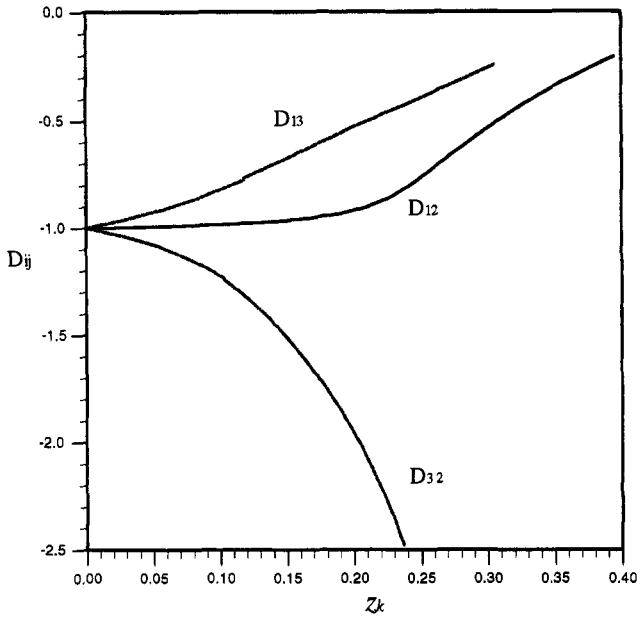

Figure 14. Path line of D_{ij} versus z_k in a type 3 case. The three lines represent three path lines from different starting points. This diagram results from using the same model as for Figure 13.

Although the examples presented in this work are all excess Gibbs energy models, this method can be applied to the EOS/MCR model. For the EOS/MCR model, Radzyminski and Whiting (1987) have noted that the different volume roots of the EOS cause a cusp in $\Delta_m G$ for vapor–liquid equilibria. The cusp then creates a jump discontinuity in the derivative of $\Delta_m G$. The equal area rule method can be used as two equal areas still exist at equilibrium (Eubank and Hall, 1994).

Conclusions

In phase equilibrium calculations from any background model, the convergence procedure becomes more complicated when the number of components and/or the number of phases increase. Conventional K-value methods may fail in cases where poor initial guesses are used or the assumed number of phases is wrong. Several techniques using Gibbs energy minimization may be used to correct such problems.

Here, we extend the equal area rule (EAR), one type of Gibbs energy minimization method, to ternary systems of two and three phases. A general algorithm to extend this method to multicomponent systems is presented. The EAR is successful in describing equilibrium loci, metastable lines, and three-phase compositions. For multicomponent and multiphase systems, the simplicity and higher computer speed of EAR have been shown to be especially superior to other Gibbs minimization procedures. When used with the D_{12} vector tie-line approach, presented here, EAR is reduced to a series of pseudobinary calculations involving only a one-dimensional search for D_{12} to obtain equilibrium compositions in ternary systems.

Future extensions of this work involve quaternary systems which can be represented by a composition tetrahedra. Here the tie-line vector $\bar{D}_{ij}$ has two components (D_{12}, D_{13}) causing a two-dimensional search to solve the isothermal, isobaric flash. Additional components (≥ 5) are important in many applications, such as petroleum reservoir modeling where the "oil" is represented by pseudocomponents plus CO_2 and water may also be present. Additional fluid phases (>3) are not so common in chemical and petroleum applications but can be treated by extension of the present techniques. Additional phases lead to additional positive and negative areas on the EAR graph (dg/dx_1 versus x_1) but some simplification results from one less degree of freedom under the phase rule of Gibbs (Eubank et al., 1995).

Acknowledgment

This research was sponsored by the National Science Foundation (Grant CTS-93), the U.S. Department of Energy (Grant DE-FG03-93AR14357), Texaco (E and P Technology), Marathon Oil Company, Chevron Oil Company, and the Center for Energy and Mineral Resources of Texas A&M University.

Nomenclature

a = parameters in the model of eq 23
D = slope of the tie line for $n \geq 3$
EAR = equal area rule
EOS = equation of state
G = Gibbs energy
$\Delta_m G$ = Gibbs energy of mixing
$g = (\Delta_m G/RT)$, dimensionless Gibbs energy of mixing
$g'_1 = (\partial g/\partial x_1)_{T,P}$, binary case
$g'_1 = (\partial g/\partial x_1)_{T,P,x_2}$
$g'_2 = (\partial g/\partial x_2)_{T,P,x_1}$
g^α, g^β = Gibbs free energy at the compositions x_1^α, x_1^β, respectively
GEM = Gibbs energy minimization
h = local composition factor for the NRTL model in eq 24
k = iteration number
MCR = mixture combining rule
MEAR = Maxwell equal area rule
P = pressure
R = gas constant
T = temperature
VLE = vapor–liquid equilibrium
VLLE = vapor–liquid–liquid equilibrium
x_1^α, x_1^β = lower and higher equilibrium compositions, for the first component in the two-phase region, respectively
z_i = overall composition of component i in a system

Greek Letters

α = NRTL model parameter, eq 25
τ = NRTL binary interaction parameter, eq 25

Superscript

E = excess property

Subscripts

1, 2, 3 = component 1, 2, 3
i, j = molecular species
m = mixture
min, max = minimum or maximum, respectively

Literature Cited

Alvarado, J. J. Studies on Phase Equilibrium Calculations from Equation of State. Ph.D. Dissertation, Texas A&M University, College Station, TX, 1993.

Ammar, M. N.; Renon, H. The Isothermal Flash Problem: New Methods for Phase Split Calculations. *AIChE J.* **1987**, *33*, 926–939.

Baker, L. E.; Pierce, A. C.; Luks, K. D. Gibbs Energy Analysis of Phase Equilibria. *Soc. Pet. Eng. J.* **1982**, Oct, 731–741.

Cairns, B. P.; Furzer, I. A. Multicomponent Three-Phase Azeotropic Distillation. Part II. Phase-Stability and Phase-Splitting Algorithms. *Ind. Eng. Chem. Res.* **1990**, *29*, 1364–1382.

Eubank, P. T.; Hall, K. R. An Equal Area Rule and Algorithm For Determining Phase Compositions. *AIChE J.* **1995**, *41*, 924–927.

Eubank, P. T.; Elhassan, A. E., Barrufet, M. A.; Whiting, W. B. Area Method for Prediction of Fluid Phase Equilibria. *Ind. Eng. Chem. Res.* **1992**, *31*, 942–949.

Eubank, P. T.; Hanif, N. S.; Shyu, G.-S.; Hall, K. R. Application of EAR to the Calculation of Multi-Phase Equilibria of Hydrocarbon/Water Mixures. *Fluid Phase Equilib.* **1995**, in press.

Gautam, R.; Seider, W. D. Computation of Phase and Chemical Equilibrium. Part I. Local and Constrained Minima in Gibbs Free Energy. *AIChE J.* **1979**, *25*, 991–999.

Heidemann, R. A. Three-Phase Equilibria using Equations of State. *AIChE J.* **1974**, *20*, 847–855.

Hicks, C. P.; Young, C. L. Theoretical Prediction of Phase Behavior at High Temperatures and Pressures for Non-Polar Mixtures: Computer Solution Techniques and Stability Tests. *J. Chem. Soc., Faraday. Trans.* **1977**, *2* (73), 597.

Kao, Y.-K. Separation Vector: A New Method to Represent and Measure Separation. *Chem. Eng. Commun.* **1992**, *118*, 279–298.

Kao, Y.-K. Separation Vector Formulation for the Synthesis of Multicomponent Separation Sequences. *AIChE J.* **1995**, *41*, 78–96.

Michelsen, M. L. The Isothermal Flash Problem. Part I. Stability. *Fluid Phase Equilib.* **1982a**, *9*, 1–19.

Michelsen, M. L. The Isothermal Flash Problem. Part II. Phase-Split Calculation. *Fluid Phase Equilib.* **1982b**, *9*, 21–40.

Radzyminski, I. F.; Whiting, W. B. Fluid Phase Stability and Equations of State. *Fluid Phase Equilib.* **1987**, *34*, 101–110.

Rowlinson, J. S.; Swinton, F. L. *Liquids and Liquid Mixtures*, 3rd ed.; Butterworth: London, 1982; p 121.

Trangenstein, J. A. Minimization of Gibbs Free Energy in Compositional Reservoir Simulation. *Soc. Pet. Eng. J.* **1985**, Sept, 233–246.

Sørensen, J. M.; Arlt, W. *Liquid-Liquid Equilibrium Data Collection; Ternary Systems; DECHEMA Data Series*; DECHEMA: Frankfurt, 1977; Vol. V, Part 2.

Walas, S. M. *Phase Equilibria in Chemical Engineering*; Butterworth: Boston, 1985; pp 281–292.

Received for review March 22, 1995
Revised manuscript received August 11, 1995
Accepted August 31, 1995[⊗]

IE950192K

[⊗] Abstract published in *Advance ACS Abstracts,* November 15, 1995.